Chapter 3

Nanoscale Fabrication and Characterization

In this chapter, we discuss typical techniques for the fabrication and characterization at the nanometer scale. These techniques provide the experimental bases for the research and development of nanoscience and nanotechnology.

3.1 Nanoscale Fabrication

Various fabrication processes have been developed and applied for nanoscale fabrication [1-4]. Usually, the selection of a fabrication process is based on the requirement and the type of nanomaterials to be fabricated. As shown in Figure 3.1, there are two general approaches for nanoscale fabrication: top-down and bottom-up.

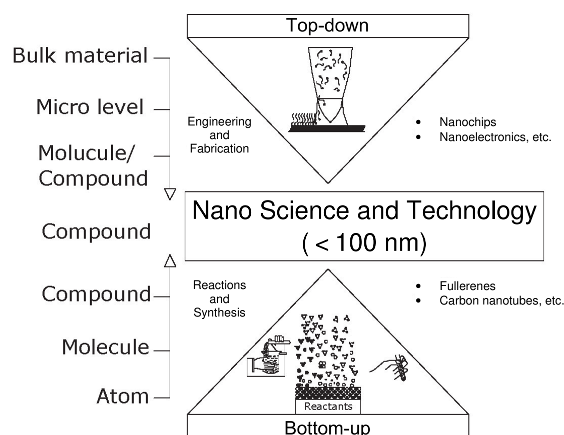

Figure 3.1 Top-down and bottom-up approaches for nanoscale fabrication.

The bottom-up approach has the following features. First, materials are synthesized from atomic or molecular species via chemical reactions. Second, chemical and biological reactors create conditions for special growth and assembly. Third, materials can self-assemble together to form more complex modules. Fourth, materials containing regular nano-sized pores can be used as templates for synthesizing nanoparticles, nanowires and nanotubes. Nanostructures fabricated with the bottom-up approach usually have less defects, more homogeneous chemical composition. The bottom-up approach is driven mainly by the reduction of Gibbs free energy, so that the nanomaterials produced are in a state closer to a thermodynamic equilibrium state.

The top-down approach has the following features. First, this approach breaks bulk materials into smaller sizes using lithography, mechanical and chemical manipulation tools. Second, optical, electron or ion beams are used for generating nanoscale patterns over a surface. Third, high precision actuators are used to move atoms or molecules from place to place. Fourth, micro tips are used to emboss or imprint materials. Top-down approach most likely introduces internal stress, in addition to surface defects and contaminations.

In the following, we discuss typical techniques for the bottom-up approach and top-down approach. More discussions about these two approaches can be found in Chapter 5.

3.1.1 *Bottom-up approach*

Three techniques are often used in the bottom-up approach: chemical synthesis, self-assembly and positional assembly. Usually, a large number of atoms, molecules or particles are used or created by chemical synthesis, and then arranged into desired structures.

3.1.1.1 *Chemical synthesis*

Chemical synthesis is often used for producing raw materials, such as molecules or particles. These raw materials can be used directly in products in their bulk disordered form, and they can also be used as building blocks for more advanced materials. In this technique,

individual atoms or molecules are placed or self-assembled precisely to the places where they are needed. The chemical synthesis of various types of carbon nanomaterials is discussed in Chapter 4.

3.1.1.2 *Self-assembly*

In this technique, atoms or molecules arrange themselves into ordered nanoscale structures by physical or chemical interactions between the units. Typical examples of self-assembly include the formation of salt crystals and snowflakes with intricate structures. In some cases, an external force or field, for instance, electric or magnetic field, is applied to accelerate a slow self-assembly process. This technique is called directed self-assembly, and is often used in industries.

Based on different working mechanisms, different self-assembly processes have been developed, including chemical self-assembly, physical self-assembly and colloidal self-assembly. Chemical self-assembly converses molecular scale ordering of compounds with precisely designed atomic structures into more macroscopic structures. Physical self-assembly refers to the ordering of atoms that results from deposition processes, such as molecular beam epitaxy or chemical vapor deposition. By colloidal self-assembly, nanoparticles may aggregate into clusters.

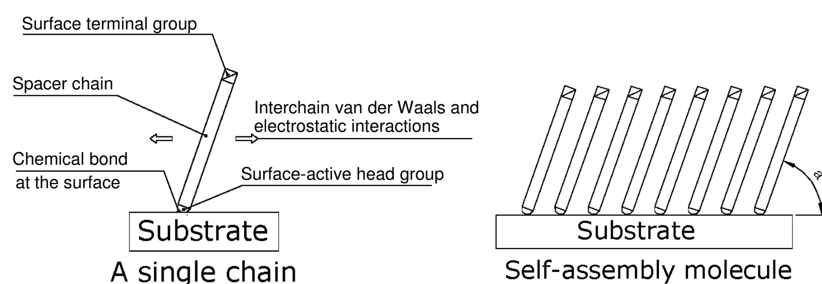

Figure 3.2 Building groups of self-assembly monolayers.

Self-assembly monolayers (SAM) are formed as a result of spontaneous self-organization of functionalized organic molecules onto the surfaces of appropriate substrates into stable, well-defined structures.

The final structure is close to or at thermodynamic equilibrium and it rejects defects. As shown in Figure 3.2, SAMs consist of three building groups: a head group (binding to a substrate), a surface terminal group, a spacer chain (backbone chain).

3.1.1.3 *Positional assembly*

In this technique, atoms, molecules or clusters are deliberately manipulated and positioned one-by-one. Usually, this technique needs scanning probe microscopes for working on surfaces, and optical tweezers for working in free space. At present, this technique is laborious, and is not suitable for industrial processes.

3.1.2 *Top-down approach*

The most popular top-down technique is nanolithography. In a conventional lithography process, materials are either deposited or removed on a substrate. The specific pattern developed on the substrate surface may lead to the changes in various properties, such as electrical, optical, etc., at that specific location depending the materials used [5, 6]. As shown in Figure 3.3, in a process of spin coating of photoresist layer, polymer goes on wet, and is then dried after spinning. The thickness of the material deposited depends on the spin speed of the spin coater and the viscosity of the photoresist.

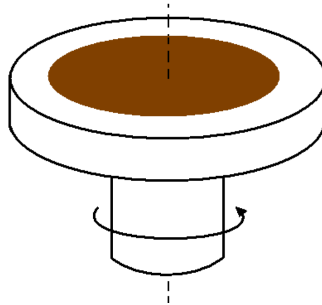

Figure 3.3 Spin coating of photo resist layer.

Nanolithography involves with the etching, writing or printing at the microscopic level on the order of nanometers. This technique may also be considered as a hybrid approach, since the growth of thin films is bottom-up whereas etching is top-down approach. The scanning probe microscopy (SPM) and the atomic force microscopy (AFM) are often used in nanolithography. By using the SPM, a surface can be viewed in fine details without modifying it. Both the SPM and the AFM can be used to etch, write or print on a surface in single-atom dimensions. In the following, we discuss typical lithography techniques.

3.1.2.1 *Photolithography*

As shown in Figure 3.4, photolithography, also called optical lithography, transfers a pattern from a photomask to the surface of a substrate. This technique is widely used for the fabrication of semi-conductor devices.

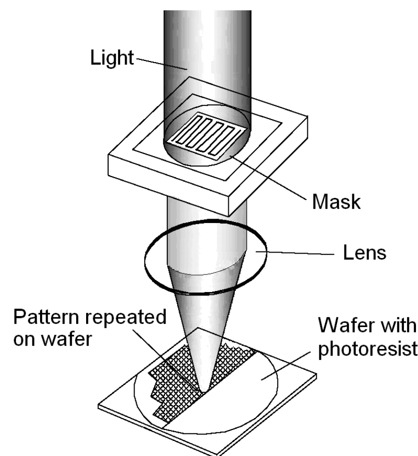

Figure 3.4 Schematic diagram showing a projection photolithography. (Image courtesy of Semiconductor Industry Association, with modifications made.)

Among various approaches for photolithography, projection lithography is the most commonly used. In this approach, the desired pattern is projected from the photomask onto the wafer. As shown in Figure 3.4, a light passes through a mask containing the desired image,

and is then focused to produce the desired image on the wafer through a reduction lens system.

In this technique, the entire surface is drawn at a single moment, so this technique is a parallel method of nanolithography. Usually the substrates used are silicon wafers, and other options mainly include glass, sapphire and metal. However, if the wavelength of light used is extremely short, the lens may totally absorbs the light. This means that photolithography cannot reach the resolutions of some alternate technologies.

A full photolithography procedure involves a combination of substrate preparation, photoresist application, soft-baking, exposure, developing, hard-baking, etching and other chemical treatments in repeated steps on an initially flat substrate. A typical silicon lithography process would start with depositing a layer of conductive metal several nanometers thick on the substrate. Then a layer of photoresist is applied on top of the metal layer. After that, a photomask is placed between a source of illumination and the wafer, selectively exposing parts of the substrate to light. The photoresist is subsequently developed, and in this procedure the unhardened photoresist undergo a chemical change. After hard-baking, the conductor under the developed photoresist is etched away. Finally, the hardened photoresist is etched away, leaving the conductor in the pattern of the original photomask.

This technique requires extremely clean operation conditions. Besides, this technique is not very effective for creating shapes that are not flat.

3.1.2.2 *Electron beam lithography*

Electron beam lithography (EBL) allows for smaller sizes than photolithography. In this technique, an electron beam is used to generate patterns on a surface, and extremely small sizes on the order of nanometers can be achieved. This technique is one of the ways to beat the diffraction limit of light, and it has been used in industry, mainly for generating exposure masks to be used in conventional photolithography.

The task of EBL is to expose a pattern and remove, by etching or dissolution, the exposed portion of the polymer resist film. Due to the

exposure, the molecular linear chains of the polymer on the exposed area are broken, and thus their average molecular weight is reduced. The reduction in the molecular weight of the polymer causes an increase of the solubility, which is related to the etching rate. Therefore a pattern drawn in terms of etching rate is obtained after the exposure, and it is desired that the contrast be as large as possible. The principle of EBL is shown schematically in Figure 3.5. This system has a high-speed electron gun which emits electrons, and the substrate is placed on a platform.

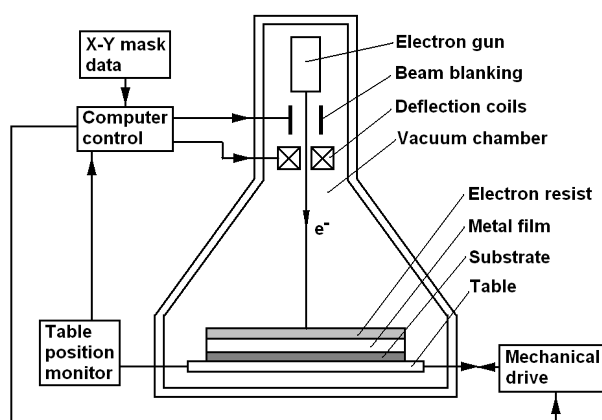

Figure 3.5 Schematic diagram of EBL process.

Based on current technology in electron optics, electron beam widths can go down to several nanometers, and this limit is mainly due to aberrations and space charge. However the practical resolution limit in BEL is mainly determined by forward scattering in the photoresist and secondary electron travel in the photoresist. Though the forward scattering could be decreased by using thinner photoresists and electron beams with higher energy, the generation of secondary electrons is inevitable.

Generally speaking, EBL is much more expensive and time consuming than photolithography. A job that takes one minute using photolithography would take more than one hour with electron-beam lithography.

3.1.2.3 *Focused ion beam lithography*

Combined with high-performance scanning electron microscopy (SEM), the focused ion beam (FIB) lithography technology is making a big impact on nanotechnology, particularly with the ability to use either focused ions or electrons to perform advanced nanolithography.

Figure 3.6 illustrates the basic operating principle of an FIB system. The focused ion beam instrument is similar in principle to an SEM. However, instead of using an electron beam to irradiate the sample, a beam of gallium ions is used. The instrument consists of the ion beam source, a set of electrostatic lenses and a scanning system, which allows the ion beam to be scanned over the surface of the sample with nanometer precision. The ion beam is generated in a liquid-metal ion source, and the application of a strong electric field causes emission of positively charged ions from a liquid gallium cone, which is formed on the tip of a tungsten rod. As illustrated in Figure 3.6, modern FIB systems involve the transmission of a parallel beam between two lenses. A set of apertures are used to select the beam current and hence the beam size and image resolution. The beam energy is typically in the range of 30 to 50 keV with a beam current in the range of 1 to 20 nA, and the best image resolution that can be obtained is approximately 5-7 nm.

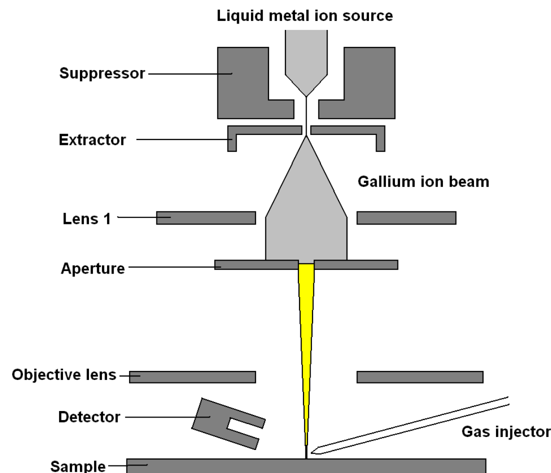

Figure 3.6 Basic principle of FIB equipment.

In the lithography process, the beam is raster-scanned over the sample, which is mounted in a vacuum chamber at a pressure of around 10^{-7} mbar. When the beam strikes the sample, secondary electrons and secondary ions are emitted from its surface. The electron or ion intensity is monitored and used to generate an image of the surface. Secondary electrons are generated in much greater quantities than ions and provide images of better quality and resolution. Therefore the secondary electron mode is used for most imaging applications.

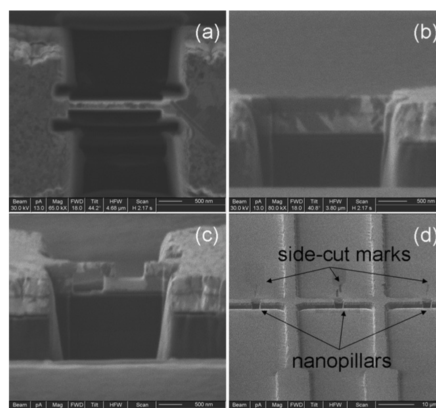

Figure 3.7 FIB micrograph of the nanopillar: (a) top view before lateral milling, (b) side view before lateral milling, (c) a completed nanopillar device and (d) low-magnification image of three nanopillars. Source: Wu, M. C., Aziz, A., Witt, J. D. S., Hickey, M. C., Ali, M., Marrows, C. H., Hickey, B. J. and Blamire, M. G. (2008). Structural and functional analysis of nanopillar spin electronic devices fabricated by 3D focused ion beam lithography, *Nanotechnology*, **19**, 485305. IOP Publishing Ltd.

Besides the conventional ion beam ligthography, three-dimensional (3D) focused ion beam lithography process has been developed, and used in the fabrication of 3D nanostructures and nanodevices [21]. Figure 3.7 shows a nanopillar fabricated by the 3D focused ion beam lithography process. This process exhibits two attractive advantages: firstly, this process preserves excellent interface cleanliness throughout the structure as all layers, including the electrodes, are deposited in a single ultrahigh vacuum process; secondly this process creates accurately rectangular devices rather than the more conventional circular or elliptical structures achieved by e-beam patterning. The former is important in eliminating

the parasitic resistances and heating, and the latter enables accurate modeling of the device behavior [21].

Ion beams can also be used to remove material from the surface of the sample. This process, called milling, is a major advantage of FIB as much of the constructional analysis and failure analysis of semiconductor devices is performed on cross-sections. In a typical cross-sectional analysis, a crater is milled in the sample and the imaging is performed on the originally vertical wall of the crater after tilting the sample, generally by 45°. These craters are usually 15-20 µm wide and are milled in several steps. The initial crater has a stair case shape and is created using a strong beam current. The final milling of the wall is accomplished using line scans with a low beam current, so that the face obtained is flat and steep.

Similar to other analytical techniques, FIB analysis also has its drawbacks. Major problems include the damage to the milled surfaces from ion implantation, and the fact that some milling will occur during the imaging process. This milling slowly degrades the quality of the images. The latter problem can be avoided by using dual-beam FIB systems. These combine an FIB and an SEM column where the ion beam can be used for milling and the electron beam for imaging.

3.1.2.4 *Dip-pen nanolithography*

Dip-pen nanolithography (DPN) is a direct write lithographic technique that uses an AFM to build a pattern on the substrate material rather than etching it away. In the same way that an old fashioned dip-pen picks up ink from an ink well and then writes on a paper, in DPN, molecules are picked up from a reservoir on the end of the AFM tip and deposited to the surface of the substrate via a solvent or water as shown in Figure 3.8.

In order to create stable nanostructures, it is beneficial to use molecules that can anchor themselves to the substrate via chemisorption or electrostatic interactions. DPN can be used for both fabrication and imaging. This technique can be used to create patterns with resolutions down to 10 nm. Dip-pen nanolithography can be used in a range of applications from semiconductor patterning and chip manufacturing to biomedical and pharmaceuticals development.

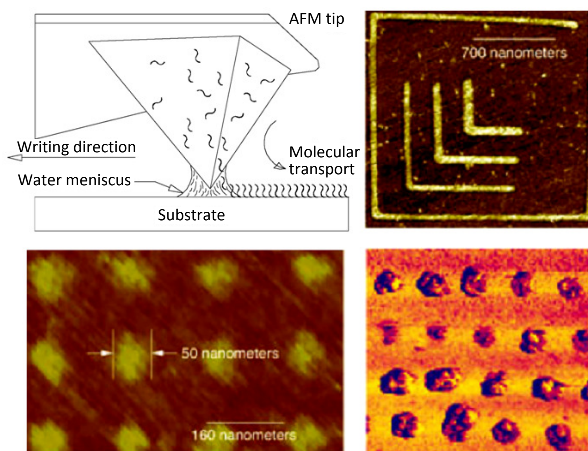

Figure 3.8 Schematic diagram showing how dip-pen nanolithography works. Several patterns obtained by DPN are also shown. Source: https://www.llnl.gov/str/December01/Orme.html.

3.1.2.5 *Extreme ultraviolet lithography*

Extreme ultraviolet lithography (EUVL) is similar to standard photolithography except that it uses intense beams of ultraviolet light reflected from a circuit design pattern, or mask, to burn the pattern into a silicon wafer [7]. It is an emerging contender for the replacement of optical photolithography in many areas. As all matters absorb extreme ultraviolet (EUV) radiations, EUVL should be performed in a vacuum. All the optical elements, including the photomask, must make use of defect-free Mo/Si multilayers which reflect light by means of interlayer interference, and each of these mirrors will absorb around 30% of the incident light. However, in a maskless interference lithography system, this limitation can be avoided, but such a system is restricted to producing periodic patterns only.

Figure 3.9 shows an EUVL apparatus [23]. In this system, the EUV is generated by the focused plasmas of laser or discharge pulses. The mirrors are responsible for collecting the light. When EUV photons are absorbed, photoelectrons and secondary electrons are generated by ionization, and this is similar to what happens when X-rays or electron beams are absorbed by a matter. These secondary electrons have energies

in the range of a few to tens of eV, and travel tens of nanometers inside photoresist before initiating the desired chemical reaction. Usually EUV photoresist images require resist thicknesses close to the wavelength.

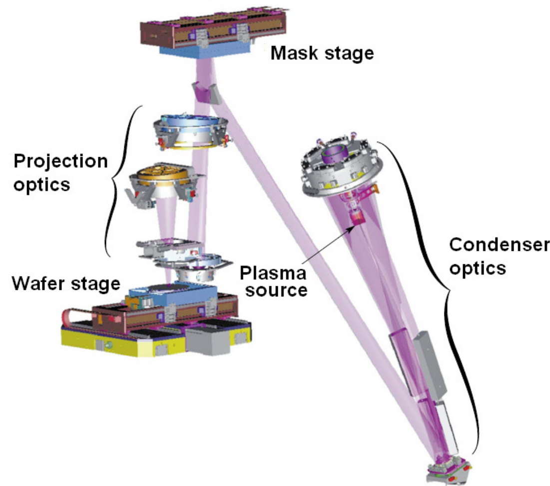

Figure 3.9 The optical layout of the engineering test stand for EUVL. Source: Sweeney, D. (1999). Extreme ultraviolet lithography: imaging the future, Science and Technology Review, November, 4-9. (Image courtesy of Lawrence Livermore National Laboratory, U.S. Department of Energy's National Nuclear Security Administration).

3.1.2.6 *Nanoimprint lithography*

Nanoimprint lithography is a novel method for the fabrication of nano scale patterns [8-10]. It is a simple process with high resolution, high throughput and low cost. The working principle of nanoimprint lithography (NIL) is similar to a rubber stamp. In this technique, a rubber-like polymer is inscribed a pattern, and its surface is coated with molecular ink. Then the ink is stamped out onto a surface, such as metal, polymer, oxide and other surface. In this process, patterns can be imprinted on micro and nano levels. It has a variety of applications such as single electron transistor device fabrication, fluidic channel fabrication, bio-molecule patterning for biosensors, polymeric material processing, pattering organic semiconductors for OLED and FET and polymer based MEMS and NEMS device.

There are two types of nanoimprint lithography processes: thermoplastic nanoimprint lithography and photo nanoimprint lithography.

(1) *Thermoplastic nanoimprint lithography*

In a thermoplastic nanoimprint lithography (T-NIL) process, a thin layer of imprint resist (thermoplastic polymer) is spin coated onto the sample substrate. In the procedure of T-NIL shown in Figure 3.10, a layer of prepolymer is deposited over the master. By heating up the polymer above its glass transition temperature, the pattern on the master is pressed into the melt polymer film [11]. After polymerization, an elastomeric stamp is obtained. The printing is then carried out using ink solution. A pattern transfer process, for instance, reactive ion etching, can be used to transfer the pattern in the resist to the underneath substrate.

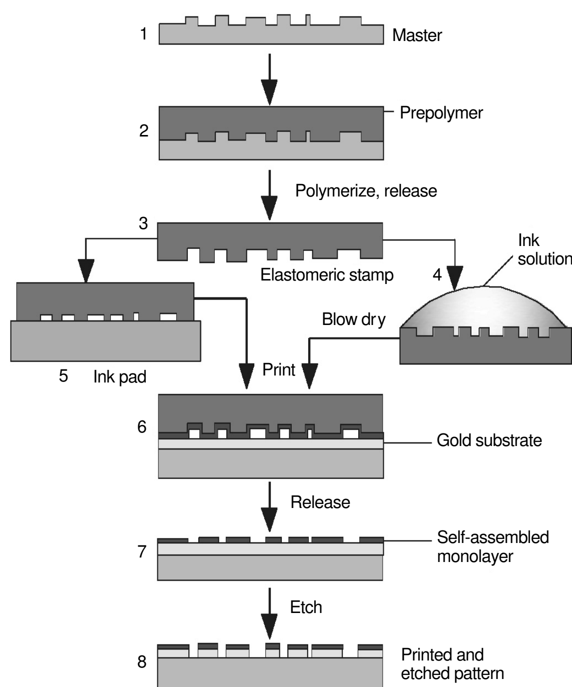

Figure 3.10 Procedure of nanoimprint lithography [11].

(2) *Photo nanoimprint lithography*

In a photo nanoimprint lithography (P-NIL) process, a photo (UV) curable liquid resist is applied to the substrate, and usually the mold is made of transparent material, such as fused silica. After the mold and the substrate are pressed together, the liquid resist is cured by UV light and becomes solid. After the mold is separated, the pattern in resist is transferred onto the underneath material by a pattern transfer process. Usually the resist is a monomer or polymer which is cured by UV light during the imprinting procedure, and the adhesion between the resist and the mold is controlled to ensure proper release. This process is schematically shown in Figure 3.11.

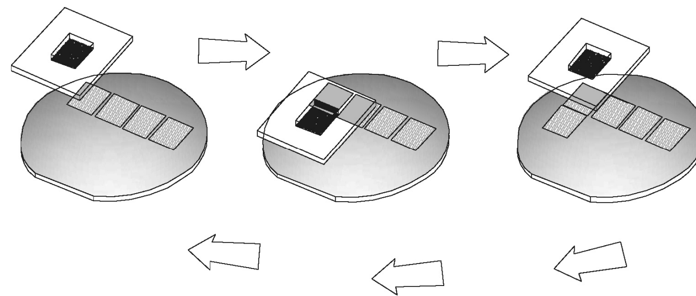

Figure 3.11 Photo nanoimprint lithography process [24].

There are two schemes of photo nanoimprint lithography: full wafer nanoimprint scheme, and step and repeat optical lithography. In the full wafer nanoimprint scheme, all the patterns are contained in a single nanoimprint field and transferred in a single imprint step. Using this scheme, high throughput and uniformity can be achieved. In the step and repeat nanoimprint scheme, nanoimprint is performed in a way similar to the step and repeat optical lithography. The imprint field (die) is typically much smaller than the full wafer nanoimprint field, and the imprinting to the substrate is repeated with a certain step size. This scheme is ideal for the creation of nanoimprint molds.

Nanoimprint lithography is widely used in fabricating devices for various applications. In electronics, NIL can be used to fabricate MOSFET, O-TFT, single electron memory. In photonics and optics, this

technique can be used in the fabrication of subwavelength resonant grating filter, polarizers, anti-reflective structures, integrated photonics circuit and so on. In biology, NIL technique has been used to fabricate sub-10 nm nanofluidic channels that can be used in DNA diagnosis, and this technique can also be used in miniaturizing various biomolecular sorting devices.

Nanoimprint lithography is a simple and inexpensive technique. This technique does not require complex optics or high-energy radiation sources. There is no need for photoresists finely tailored for resolution and sensitivity at a specified wavelength. Furthermore, since large areas can be imprinted in one step, this is also a high-throughput technique.

3.1.2.7 *Contact lithography*

This technique is also called contact printing. In this technique, the image to be printed is obtained by illumination of a photomask which is in direct contact with a substrate coated with a layer of photoresist. This technique is a candidate for sub-45 nm semiconductor lithography.

The chief advantage of contact lithography is the elimination of the need for complex projection optics between object and image. The resolution limit in today’s projection optical systems originates from the finite size of the final imaging lens and its distance from the image plane. More specifically, the projection optics can only capture a limited spatial frequency spectrum from the object (photomask). Contact printing has no such resolution limit but is sensitive to the presence of defects on the mask or on the substrate.

However, due to the photomask-photoresist interface, the image-forming light is subject to near-field diffraction as it propagates through the photoresist. Because of the diffraction, the image contrast will decrease with increasing depth into the photoresist. By using a thinner photoresist, this effect can be partly alleviated.

3.1.2.8 *X-ray lithography*

X-ray lithography is a next generation lithography developed for the semiconductor industry [12-14]. In this technique, collimated X-rays

are used as the exposing energy. The short wavelengths of X-rays overcome the diffraction limits in the resolution of conventional optical lithography. As shown in Figure 3.12, X-rays illuminate a mask placed near to a wafer coated with a layer of resist, and no lenses are used. The mask used in X-ray lithography consists of an X-ray absorber on a membrane that is transparent to X-rays [15]. Typically, the material for the X-ray absorber is gold or compounds of tantalum or tungsten, and the material for the membrane is silicon carbide or diamond. The pattern on the mask is written by electron beam lithography onto the resist coated on the wafer.

Typically, the X-rays used in this technique are generated by a compact synchrotron radiation source, and their wavelengths are around 0.8 nm. To perform deep X-ray lithography, X-rays with shorter wavelengths, about 0.1 nm, are needed. With modified procedures, deep X-ray lithography can be used to fabricate deeper structures, even three-dimensional structures.

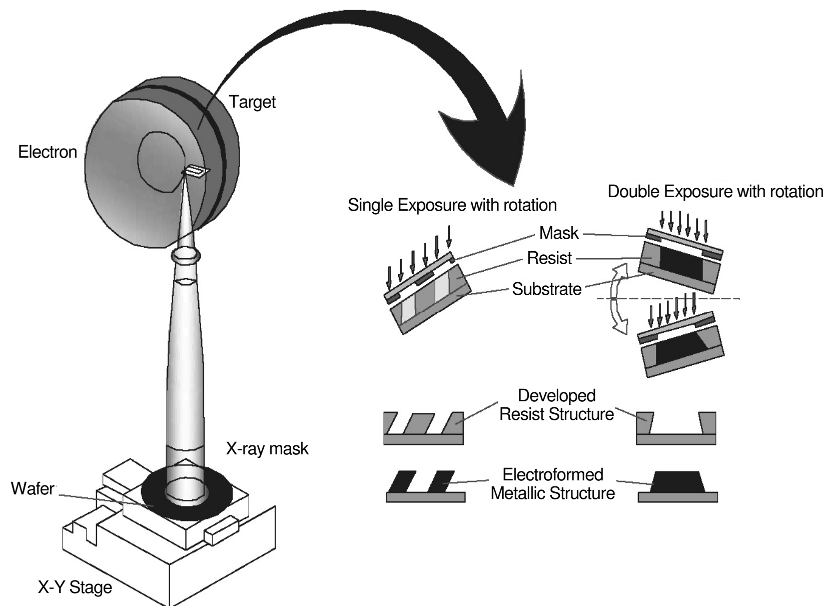

Figure 3.12 Schematic view of X-ray lithography (MIRRIRCLE – 20SX, Photon Production Laboratory). [25]

3.1.2.9 *Lift-off lithography*

Lift-off lithography is a technique to fabricate nanostructures by taking advantage of the AFM tip sharpness. A narrow furrow is engraved in a soft polyimide layer. The furrow is then transferred using dry etching to a thin germanium layer which forms a suspended mask. Metallic layers are then evaporated through this mask. Using this technique, metallic lines with line width in nanometers and single-electron transistors can be fabricated. Figure 3.13 schematically shows the typical process of lift-off lithography [22].

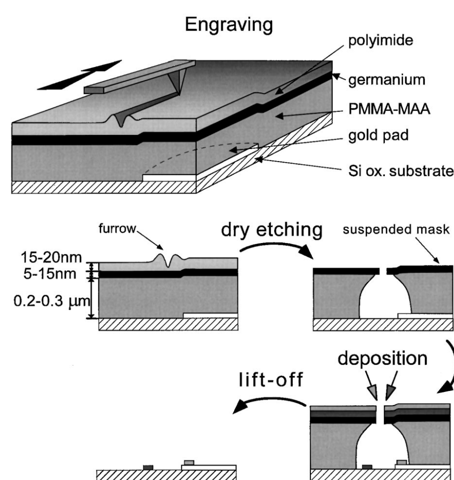

Figure 3.13 Main steps of the AFM-based trilayer process. Reprinted with permission from: Bouchiat, V. and Esteve, D. (1996). Lift-off lithography using an atomic force microscope, *Applied Physics Letters*, **69** (20), 3098-3100. © 1996, American Institute of Physics.

This technique can be used on any substrates and allows easy alignment with previously fabricated structures. One attractive feature of this technique is that many sorts of surfaces and paints (metals and molecules) can be used, and several layers of paint can be put down sequentially.

The lift-off technique can be used to produce monolayers. The fabrication of monolayers is based on the capillary force (surface tension) due to meniscus formation and the convective flow due to water

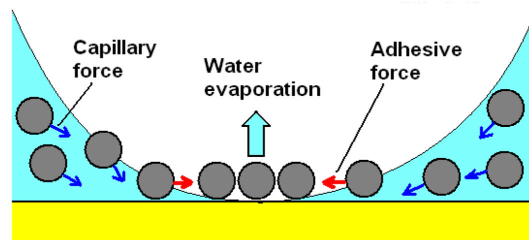

Figure 3.14 Fabrication of monolayers of polystyrene spheres [26].

evaporation. Figure 3.14 schematically shows the fabrication of monolayers of polystyrene spheres.

It should be noted that the deposition template (lift-off) approach for transferring a pattern from resist to another layer is less common than using the resist pattern as an etch mask. The main reason is that the resist is incompatible with most MEMS deposition processes, as it usually cannot withstand high temperatures and may be a source of contamination. As the resist may be incompatible with further micromachining steps, usually it is stripped once the pattern has been transferred to another layer.

3.1.2.10 *Soft lithography*

In soft lithography, structures are fabricated or replicated using elastomeric stamps, molds and conformable photomasks. The word "soft" indicates that elastomeric materials are used. This technique is often used in constructing features measured on the nanometer scale. Soft lithography includes the technologies of microcontact printing, replica molding, microtransfer molding, micromolding in capillaries and solvent-assisted micromolding.

In a typical procedure of soft lithography as schematically shown in Figure 3.15, the photoresist is applied on a clean wafer and then the master is developed using UV. This leads to the development of polydimethylsiloxane (PDMS) master and mould. PDMS is a type of soft silicone polymer. Polylactic-co-glycolic acid (PLGA) is applied over the PDMS mould, and finally PLGA of desired size and shape is obtained.

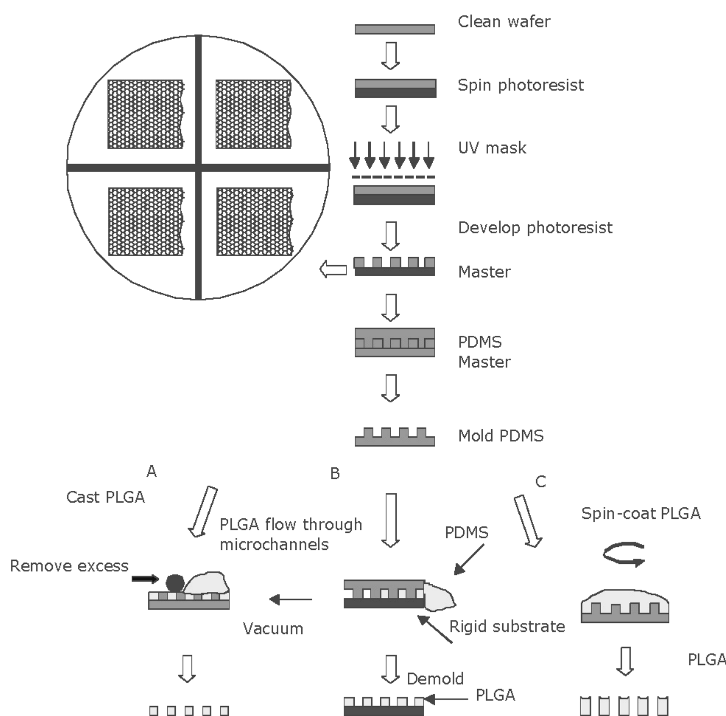

Figure 3.15 Procedure of soft lithography. Image courtesy of Center E. Piaggio [27].

This technique exhibits obvious advantages over other forms of lithography, such as photolithography and electron beam lithography. Its cost is lower than that of traditional photolithography in mass production. It does not need a photo-reactive surface to create a nano-structure, and more pattern-transferring technologies can be used in this technique. It has higher resolution than photolithography in laboratory settings (~30 nm versus ~100 nm). This technique is well-suited for applications in plastic electronics and biotechnology. Furthermore, it is well-suited for applications involving large or nonplanar surfaces.

3.2 Characterization of Nanomaterials

Characterization of nanomaterials is an area of great scientific interest as bottom-up approaches are undergoing exponential growth to fulfill a

wide range of applications such as pharmaceuticals, catalyses, coatings, optics, electronics, nanofluids, nanocomposites and tissue engineering [16, 17]. One important prerequisite for the development, manufacturing and commercialization of nanomaterials is to establish the characters of these materials before they are use. Therefore, the characterization of their physical, chemical and biological properties on a nanoscale level is crucial in nanoscicence and nanotechnology.

3.2.1 *Atomic structure and chemical composition*

The atomic structure and chemical composition of nanomaterials are the most important and the most essential characteristics for analyzing the behaviors of the nanomaterials. Though the techniques we discuss in this section are not specifically used for nanomaterials only, they can provide valuable information on the properties of nanoscale materials, which may differ significantly from those of bulk materials. Spectroscopic methods are widely used for the determination of the characteristics of nanomaterials, but they require large instruments, ultra-high vacuum and expensive sample preparation. In the following, we discuss four types of spectroscopic methods, including vibrational, nuclear magnetic resonance, X-ray and UV spectroscopies, which have been extensively used for the characterization of nanomaterials.

3.2.1.1 *Vibrational spectroscopies*

Vibrational spectroscopies comprise Fourier transform infrared (FTIR) spectroscopy and Raman scattering (RS). These two methods can be used to investigate the vibrational structures of molecules or solids. FTIR is more suitable for organic compounds and used extensively for them. Both of the methods can be performed on dry powders or liquid suspensions. For FTIR, the absorption spectra are deduced from transmission measurements through a KBr pellet with entrapped nanoparticles or directly on nanoparticles in a reflection mode measurement (DRIFT). FTIR can be also used to determine the crystallization and grain sizes of nanostructured powders and bulk materials. The principle of FTIR spectroscopy is schematically shown in Figure 3.16. In FTIR,

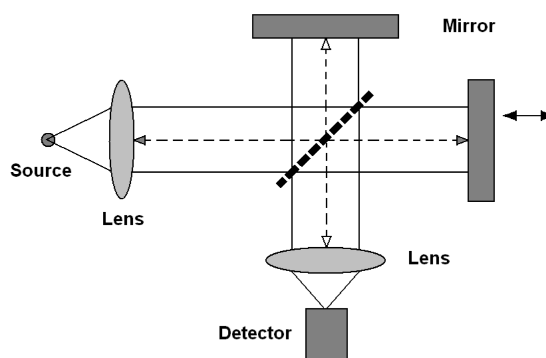

Figure 3.16 Principle of FTIR spectroscopy.

the light source is IR and the response of IR after passing through the specimen is detected by an IR detector.

3.2.1.2 *Nuclear magnetic resonance*

High resolution liquid and solid state nuclear magnetic resonance (NMR) is an important tool widely used for the characterization of nanomaterials. It can be used in identifying the elements, types of bonds, nanoscale effects, and the surface properties and chemistry of nanolayer systems. Figure 3.17 shows the working principle of NMR. Due to its spin, an electrically charged nucleus behaves like a magnet. When this nucleus is bombarded on the sample under an external magnetic field, magnetic resonance occurs. The resonance peak detected by the detector gives the information of the elements present in the nanomaterial.

3.2.1.3 *X-ray and UV spectroscopies*

X-ray and UV spectroscopies can be used to investigate the electronic structures of nanomaterials, from which their atomic structures can be deduced, such as core levels, valence and conduction band. X-ray photoemission spectroscopy (XPS) or electron spectroscopy for chemical analysis (ESCA) can be used to study the photoemission of electrons produced by a monochromatic X-ray or UV beam as shown in Figure 3.18.

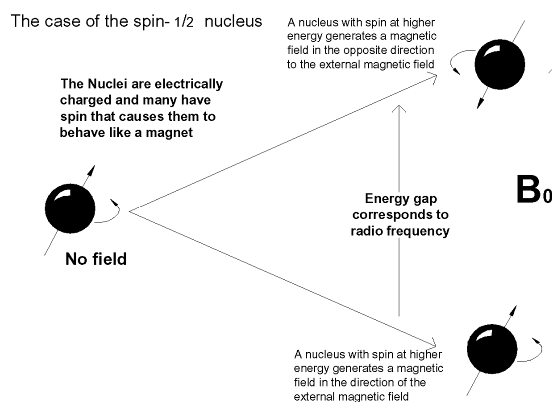

Figure 3.17 Schematic view of NMR spectroscopy. Source: Roy Hoffman and Yair Ozery, http://chem.ch.huji.ac.il/nmr/whatisnmr/whatisnmr.html. This diagram is the property of the Hebrew University of Jerusalem.

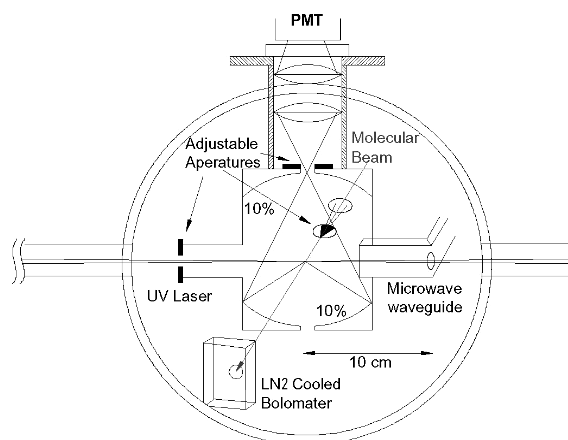

Figure 3.18 Principle of UV spectroscopy [28].

XPS techniques can be used to measure the kinetic energies of electrons. Due to the limited mean free path of the electrons in a matter, only few nanometric layers can be investigated. Since binding energies are highly sensitive to chemical bondings, a map of the bonding configuration can be obtained for surface layers. With the photoemission cross-sections, chemical compositions of the surface material can be calculated and compared to bulk chemical compositions.

X-ray absorption spectroscopy (XAS) is another X-ray method that can be used to investigate the conduction band of materials. This method involves extended X-ray absorption fine structure (EXAFS) and X-ray absorption near edge structure (XANES). The principle is based on the absorption of a monochromatic X-ray beam by a core shell electron of selected atomic species inside a sample. XAS techniques can be adapted for samples with low crystallinity. These local order techniques can be used to follow the early stages of the crystallization of amorphous nanoparticles. However, an important drawback is that XAS techniques usually require synchrotron radiation facilities.

3.2.1.4 *X-ray and neutron diffraction*

Diffraction techniques are often used to characterize the atomic structures of crystals [18]. Theoretically it is a diffraction of an incident beam (X-ray or neutrons) by the reticular planes of the crystalline phases inside a sample. As shown in Figure 3.19, the beam is diffracted at specific angular positions with respect to the incident beam depending on the phases of the sample. When the crystal size is reduced toward the nanometer scale, the diffraction peaks are broadened, and the widths of the peaks are directly correlated to the size of the nanocrystalline domains.

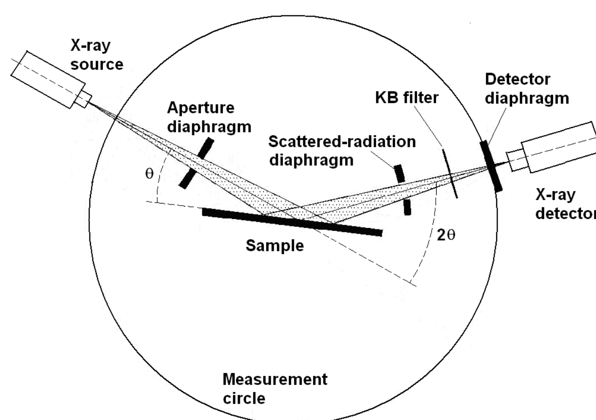

Figure 3.19 Principle of X-ray diffraction technique [29].

The X-ray and neutron diffraction techniques are extensively used for the characterization of various types of porous materials, providing quantitative parameters such as pore size, surface area and pore volume. In addition, they also allow the determination of the shape and, in particular, the spatial distribution of the pores.

3.2.2 *Size, shape and surface area*

In the research of nanoscience and nanotechnology, it is very important to characterize the size, shape and surface area of nanomaterials. In the following we discuss typical techniques for the characterization of the size, shape and surface area of nanomaterials.

3.2.2.1 *Electron microscopy*

Electron microscopies, mainly including scanning electron microscopy (SEM) and transmission electron microscopy (TEM), are powerful methods often used to investigate the properties of materials, such as

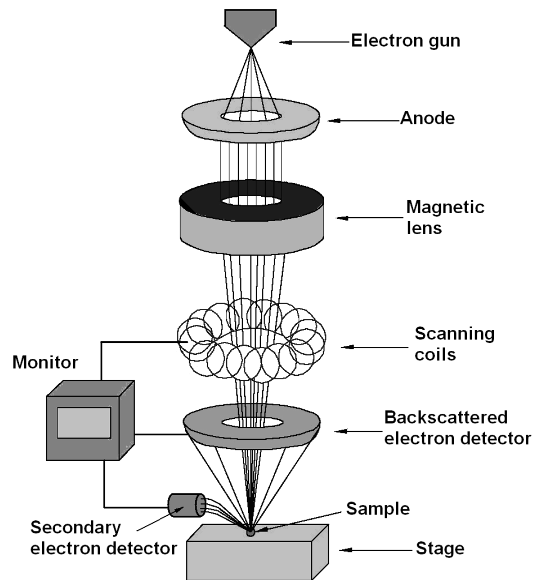

Figure 3.20 Working principle of SEM [30].

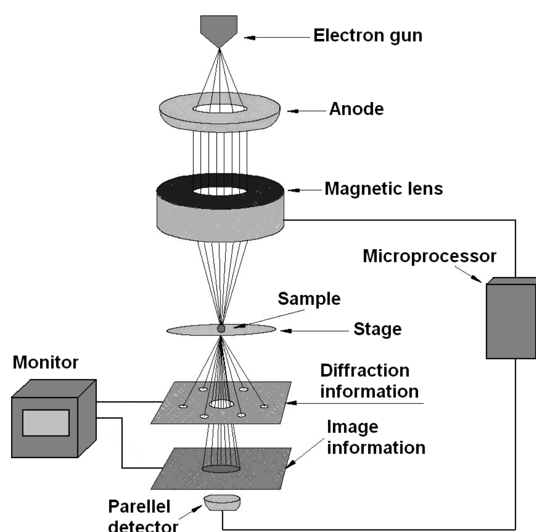

Figure 3.21 Principle of TEM [30].

size, shape and chemical composition, but the preparations of the samples for these methods are complicated. As shown in Figure 3.20, in an SEM system, electrons are produced from an electron gun, and then accelerated through anode plate and focused by magnetic lens [19]. The scanning coils force the electron beam to rapidly scan over an area of the specimen. Electrons emitted from a filament are reflected by the sample and images are formed using either secondary electrons or backscattered electrons. To investigate the nanometric scale, field emission microscope (FE-SEM) is required. FE microscopes could reach resolutions of the order of 1 nm using a cold cathode. If they are equipped with an energy dispersive spectrometer (EDS), the size distribution, shape and chemical composition of nanoparticles can be investigated by FE-SEM.

In TEM experiments, electrons pass through the sample under test and the transmitted beam is used to build the images, from which both the surface and the crystallographic information of the sample can be obtained. As shown in Figure 3.21, in a TEM system, electrons are produced from an electron gun, and then accelerated through an anode plate and focused by magnetic lens. The specimen should be very thin preferably in the order of 0.1 micrometer, so that electrons can pass

through the sample. A high resolution TEM (HRTEM) have a resolution below 1 nm, and such a high resolution can be used to observed the crystal quality and the interfaces of the sample under test.

Besides the SEM and TEM discussed above, there is another kind of electron microscopy: field emission gun scanning transmission electron microscopy (STEM). STEM combines the features of SEM and TEM. Analysis can be performed in transmission mode or in scanning mode. With STEM, electron energy loss spectroscopy (EELS) can be performed, which can be used to measure the concentration profile of nanoparticles.

3.2.2.2 *BET and pycnometry*

Specific surface area and density of nanoparticles can be obtained using the Brunauer Emmett Teller (BET) method and helium pycnometry [20]. BET and He pycnometry are performed on dry powders. Helium pycnometry is a method for measuring the true bulk density of particles if they do not contain closed pores. In helium pycnometry, the variation of the helium pressure produced by a variation of volume is studied. BET is based on the measurement of the adsorption isotherm of an inert gas at the surface of the particles. In BET, Helium and nitrogen gas are fed to chamber in which sample is placed as shown in Figure 3.22 [31]. The change in temperature is recorded by data acquisition system and the results are analyzed and extrapolated to calculate the density and surface area of the specimen.

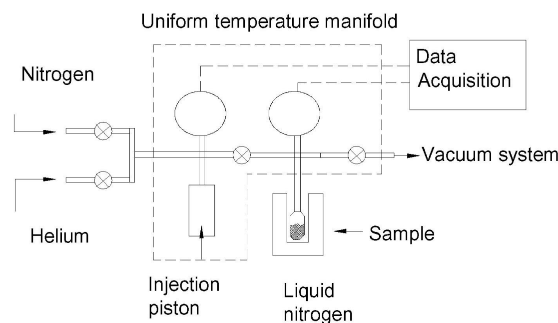

Figure 3.22 Working principle of BET method [31].

3.2.2.3 *Epiphaniometer*

An epiphaniometer is an instrument that can be used to measure the surface concentration of aerosol particles in both the nuclei and accumulation mode, and it is most sensitive to particles in the accumulation mode. Low atmospheric particle concentrations in remote locations can also be effectively measured using this method.

In this method, aerosol is passed through a charging chamber, and in the chamber, the lead isotopes created from a decaying actinium source are attached to the particle surfaces. The particles are transported through a capillary to a collecting filter. The radioactivity level of the particles collected on the filter is measured by a surface barrier detector.

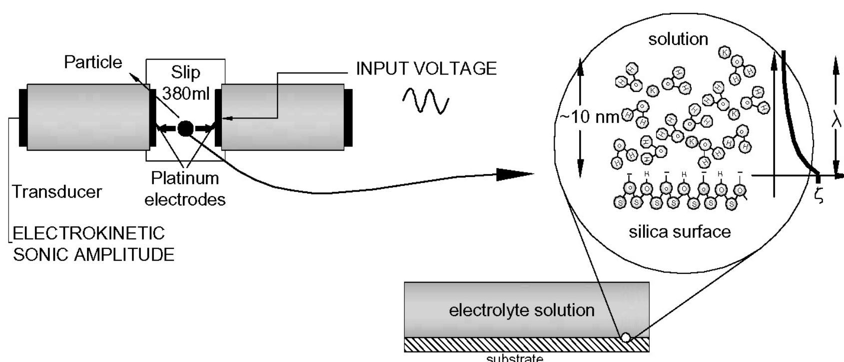

Figure 3.23 Principle of Zeta potential. Sources: Brian Kirby, Cornell University, http://www.kirbyresearch.com; and Zeta Potential, Dr. Giuliano Tari, CERAM.

3.2.2.4 *Zeta potential analyzer*

Zeta potential is a measurement of the charges carried by nanoparticles in suspensions. It is important that the liquid used should have requisite viscosity to keep nanoparticles suspended in the measurement duration. The principle of the commonly used Zeta potential analyzer is based on electrophoresis. As shown in Figure 3.23, the sample is placed between two transducers and a voltage is applied. The change in output gives a measurement of Zeta potential of the sample. Zeta potential measurements are often used to characterize the stability of the

suspensions with electrostatic repulsion. Laser granulometries, which will be discussed below, are frequently used in combination with Zeta potential analyzers.

3.2.2.5 *Laser granulometry*

Laser granulometry is a statistical method for the determination of quantitative particle size distributions. Generally speaking, there are two techniques for laser granulometry. One is based on the diffraction of a laser beam by particles in stable suspensions, and the other is based on the scattering of a laser beam by particles in stable suspensions.

In the technique based on laser diffraction, the diffraction pattern (width of the ring and intensity) is directly connected to the particles size. This technique has its own limitation that sizes lower than $\lambda/20$ are not observable. Practically, only particles with sizes higher than 80 nm can be characterized using laser diffraction.

The technique based on laser scattering can be used for smaller particles. In this technique, photon correlation spectroscopy (PCS) is used. The variations of the scattered intensities at selected angles are measured as a function of time. The scatterings are due to the Brownian motion of particles. There is an autocorrelation function which gives the changes of scattering intensity as a function of time, from which the size distribution can be derived. PCS requires the prior knowledge of solution viscosity and refractive index, and is highly sensitive to the presence of agglomerates.

3.2.2.6 *Elliptically polarized light scattering*

Based on laser light scattering, this method can be used to investigate the size distribution and the shape distribution of nanoparticles, and it also can be used to study the structure and size distribution of agglomerates. In this method, incident laser beam is elliptically polarized, and the modifications of the polarization state due to the sample are measured at specific angular positions. Polarization analysis gives complementary information about the size and structure of agglomerates. In the field of nanomaterials research and development, many properties depend upon

the agglomeration of nanoparticles. Agglomerates with size in the range between 50 nm and 2 μm can be characterized by this method.

3.2.2.7 *Gas adsorption*

A material possessing just one type of pore, even when the pores are disordered, might be more homogeneous than one having just a fraction of nicely ordered pores. Adsorption analysis is helpful for deciding and classifying porous materials according to the size of their pores. The correlation between the vapor pressure and the pore size is given by the Kelvin equation:

$$r_p\left(\frac{p}{p_0}\right)=\left(\frac{2\gamma V_L}{RT\ln\left(p/p_0\right)}\right)+t\left(\frac{p}{p_0}\right) \qquad (3.1)$$

where r_p is the pore radius, p_0 is the initial pressure, p is the final pressure, γ is the surface tension, t is the thickness of the adsorbate film, R is the Ritzberg constant, T is the temperature and V_L is the molecular volume of the condensate.

Gas adsorption method is widely used for characterizing micro and mesoporous materials, and provides porosity parameters such as pore size distributions, surface areas and pore volumes. In a typical adsorption experiment, the uptake of gases, such as nitrogen, krypton and CO_2, is measured as a function of relative pressures $p/p_0 < 1$ at a constant temperature, where p and p_0 are the equilibrium vapor pressures of the liquid in the pores and that of the bulk liquid, respectively. The interaction between the pore walls and the adsorbate is based on physisorption (van der Waals interaction) and leads to the formation of adsorbate layers at low p/p_0. Usually, the amount adsorbed on the porous solid under study is plotted as a function of the amount adsorbed on an ideal nonporous reference solid with similar surface characteristics, providing parameters such as the overall pore volume, specific surface area and micropore volumes. Gas adsorption method may be carried out using a system similar to the one for the BET method as shown in Figure 3.22.

3.2.2.8 *Positron annihilation*

Positron annihilation lifetime spectroscopy (PALS) is a powerful tool for the detection and quantification of defects on the atomic scale in various types of solids. PALS is sensitive to different kinds of defects, such as dislocations and vacancies in metals or crystals, grain boundaries, voids and pores. Similar to scattering techniques, PALS is a noninvasive technique and allows the detection of inaccessible pores. As shown in Figure 3.24, PALS is based on positron annihilation, the decay of positrons into two γ photons. With ^{22}Na as the radioactive source, the formation of positrons (β^+) by radioactive decay is accompanied by the simultaneous emergence of a γ-quantum of 1.273 MeV, which defines the starting signal of the positron lifetime measurement. If a sample is introduced, the positrons lose their high energy by inelastic collisions with electrons.

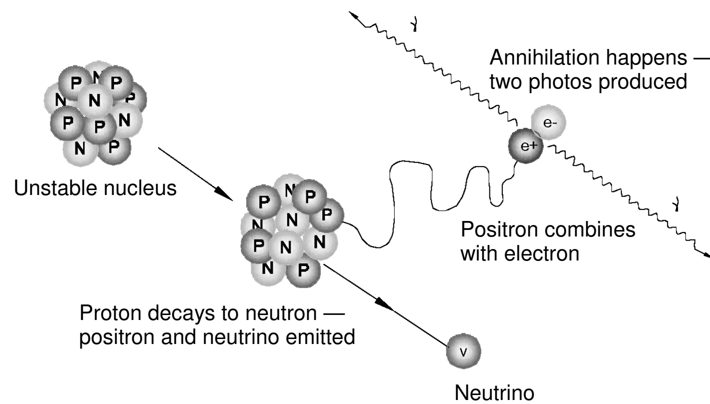

Figure 3.24 Principle of positron annihilation [32].

These "thermalized" positrons, with energies in the order of a few meV, form positroniums (Ps, the electron-positron bound state). The lifetime, the inverse of the annihilation rate, becomes longer when a positron or positronium is localized at a space with lower electron density such as a void. Therefore, positrons can be used as a probe to investigate the average sizes of the free volume, the size distribution and the free volume concentration by measuring their lifetimes.

3.2.2.9 *Mercury porosimetry*

In mercury porosimetry (MP), gas is evacuated from the sample, and the sample is then immersed in mercury. As mercury is a nonwetting fluid at room temperature for most porous materials of technological interest, an external pressure is applied to gradually force the nonwetting mercury into the sample. By monitoring the incremental volume of mercury intruded for each applied pressure, the pore size distribution of the sample can be estimated in terms of the volume of the pores intruded for a given radius r. The evaluation of pore sizes from MP is based on the Washburn equation:

$$p = \frac{2\sigma \cos\theta}{r} \tag{3.2}$$

where p is the pressure required to force a nonwetting fluid into a circular cross-sectional capillary of radius r, σ is the surface tension and θ is the wetting angle.

Mercury porosimetry allows the determination of average pore sizes in the range between 3 nm and 200 nm and their distributions. In addition, this method overestimates the volume of the smallest pores in the case of ink-bottle-shaped pores, because the intrusion of mercury into the larger pores is determined by the small openings. Moreover, it should be pointed out that pore size distributions by the Washburn equation are not a geometrical relationship, but a physical characteristic of a porous medium, because mercury porosimetry is based on transport and relaxation phenomena.

Figure 3.25 shows three main steps in mercury porosimetry. First, the sample is placed in the column which is evacuated subsequently. In next step mercury is filled. In the third step, the pressure is applied and values are taken to estimate the pore sizes.

3.2.3 *Nanoparticles in biological systems*

Most of the characterization methods discussed above are specifically meant for solid phase nanoparticles. However, on examination of biomolecules in living systems, it is found that the nanoparticles in liquid phase hold the key. If the biomolecules are examined from bottom-up

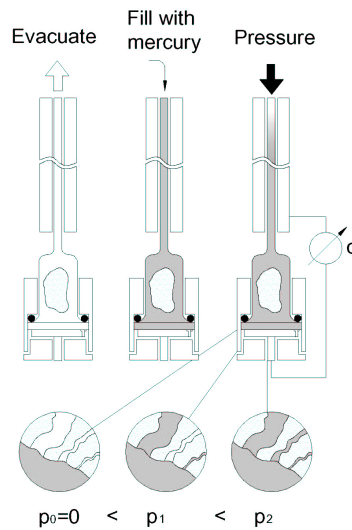

Figure 3.25 Principle of mercury porosimetry (IBP Holzkirchen, Germany).

approach of nanotechnology, it can be found that many biomolecules comprise of nanoliquids. Before nanoanalytical methods such as electron microscopy can be applied, biological samples often require complex sample preparation steps.

The transmission electron microscopy (TEM) is widely used in materials research, and is an important tool in analyzing biological macromolecules, such as proteins and viruses, on the molecular level. TEM also plays an important role in analyzing pharmaceutical, horticulture and agriculture products. There are two major problems when TEM is used for biological samples. One problem is that, since the path of the electron beam must be in vacuum, the biological sample to be observed must also be kept in vacuum. The effect of vacuum on biological specimens requires special analysis and study. The other problem is that the electron beam radiations may cause severe damage to the specimen under observation. These difficulties can be overcome by keeping the sample in the hydrated state by ice embedding method in which specimen is frozen. That is the reason why cryogenic transmission electron microscopy (Cryo-TEM) method is often used for investigating biomolecules.

Scanning transmission ion microscopy (STIM) is another important method for analyzing biological sample. This method was developed based on the idea of scanning transmission electron microscopy (STEM). In this spectroscopy, an ion beam is used instead of an electron beam which is used in STEM. The main advantage of STIM is its greater penetration depth that allows the analysis of much thicker objects. This technique makes imaging as well as mass normalization possible at resolution down to 100 nm.

Cryo-TEM and STIM are two very important methods for nanoparticle detection in biological samples, and they have been extensively used in biomedical research. For example, these methods have been applied to assess whether the nanoparticles used in cosmetics, such as creams and sunscreens, can penetrate into human skins and consequently cause systemic effects.

References:

1. Paulose, M., Varghese, O. K. and Grimes, C. A. (2003). Synthesis of gold-silica composite nanowires through solid-liquid-solid phase growth, *Journal of Nanoscience and Nanotechnology*, **3**, 341-346.
2. Chang, P. C., Fan, Z., Wang, D., Tseng, W. Y., Chiou, W. A., Hong, J. and Ju, J. G. (2004). ZnO nanowires synthesized by vapor trapping CVD method, *Chemistry Materials*, **16**, 5133-5137.
3. Park, J. Y., Lee, D. J. and Kim, S. S. (2005). Size control of ZnO nanorod arrays grown by metalorganic chemical vapour deposition, *Nanotechnology*, **16**, 2044-2047.
4. Yu, D. P., Lee, C. S., Bello, I., Sun, X. S., Tang, Y. H., Zhou, G. W., Bai, Z. G., Zhang, Z. and Feng, S. Q. (1998). Synthesis of nano-scale silicon wires by excimer laser ablation at high temperature, *Solid State Communications*, **105** (6), 403-407.
5. Cheng, X. and Guo, L. J. (2004). One-step lithography for various size patterns with a hybrid mask-mold, *Microelectronic Engineering*, **71**, 288-293.
6. Melville, D. O. S. and Blaikie, R. J. (2005). Super-resolution imaging through a planar silver layer, *Optics Express*, **13**, 2127-2134.
7. Chen F. T. (2003). Asymmetry and thickness effects in reflective EUV masks, *Proceedings of SPIE*, **5037**, 347-354.
8. Colburn, M. (2001). Development and advantages of step-and-flash imprint lithography, *Solid State Technology*, **46**(7), 67-78.
9. Choi, B. J. (2001). Distortion and overlay performance of UV step and repeat imprint lithography, *Proceedings of the Micro- and Nano-Engineering International Conference'* 2004, Rotterdam, Netherlands.

10. Cardinale, G.F. and Albert A.T. (2006). *Programmable imprint lithography template*, U. S. Patent 7,128,559.
11. Michel, B. Bernard, A., Bietsch, A., Delamarche, E., Geissler, M., Juncker, D., Kind, H., Renault, J. P., Rothuizen, H., Schmid, H., Schmidt-Winkel, P., Stutz, R. and Wolf, H. (2001). Printing meets lithography: Soft approaches to high-resolution, *IBM Journal of Research and Development*, **45** (5), 697-719.
12. Carter, D. J. D., Pepin, A., Schweizer, M. R. and Smith H. I. (1997). Direct measurement of the effect of substrate photoelectrons in X-ray nanolithography, *Journal of Vacuum Science and Technology B*, **15**, 2509-2513.
13. Vladimirsky, Y., Bourdillon, A. J., Vladimirsky, O., Jiang, W. and Leonard, Q. (1999). Demagnification in proximity X-ray lithography and extensibility to 25 nm by optimizing Fresnel diffraction, *Journal of Applied Physics D*, **32**, L114-L118.
14. Bourdillon, A. and Vladimirsky, Y. (2006). *X-ray Lithography on the Sweet Spot*, UHRL, San Jose.
15. Schattenburg, M. L., Early, K., Ku, Y. C., Chu, W., Shepard, M. I., THE, S. C., Smith, H. I., Peters, D. W., Frankel, R. D., Kelly, D. R. and Drumheller, J. P. (1990). Fabrication and testing of 0.1-mu-m-linewidth microgap X-ray masks, *Journal of Vacuum Science and Technology B*, **8** (6), 1604-1608.
16. Kruk, M., Jaroniec, M., Ryoo, R. and Kim, J. M. (1997). Monitoring of the structure of siliceous mesoporous molecular sieves tailored using different synthesis conditions, *Microporous Materials*, **12**, 93-106.
17. Gidley, D. W., Frieze, W. E., Dull, T. L., Yee, A. F., Ryan, E. T., and Ho, H. M. (1999). Positronium annihilation in mesoporous thin films, *Physical Review B*, **60**, R5157-R5160.
18. Bragg, W. H. and Bragg W. L. (1913). The reflection of X-rays by crystals, *Proceedings of the Royal Society of London. Series A*, **88**, 428-438.
19. Seiler, H. (1983). Secondary-electron emission in the scanning electron microscope, *Journal of Applied Physics*, **54**, R1-R8.
20. Brunauer, S., Emmet, P. H. and Teller, E. (1938). Adsorption of gases in Multimolecular Layers, *Journal of the American Chemical Society*, **60**, 309-319.
21. Wu, M. C., Aziz, A., Witt, J. D. S., Hickey, M. C., Ali, M., Marrows, C. H., Hickey, B. J. and Blamire, M. G. (2008). Structural and functional analysis of nanopillar spin electronic devices fabricated by 3D focused ion beam lithography, *Nanotechnology*, **19**, 485305.
22. Bouchiat, V. and Esteve, D. (1996). Lift-off lithography using an atomic force microscope, *Applied Physics Letters*, **69** (20), 3098-3100.
23. Sweeney, D. (1999). Extreme ultraviolet lithography: imaging the future, *Science and Technology Review*, November, 4-9.
24. AMO GmbH, http://www.amo.de/imprint_process.0.html?&L=1.
25. www.photon-production.co.jp/e/ppl-mirrircle-20sx.html.
26. http://jleenano.snu.ac.kr/final/?sid=312.
27. www.piaggio.ccii.unipi.it//bio/biochem/index.php?id=soft%20Lithography.htm.

28. Plusquellic, D. F. (2006). High-resolution UV spectroscopy, http://physics.nist.gov/Divisions/Div844/facilities/uvs/uvs.html.
29. http://midas.npl.co.uk/midas/content/mn027.html.
30. www.rpi.edu/dept/materials/COURSES/NANO/shaw/page5.html.
31. Jacobs, R. Basic operating principles of the Sorptomatic 1990, http://saf.chem.ox.ac.uk/Instruments/BET/sorpoptprin.html.
32. Badawi, R. (1999). *Introduction to PET Physics*, http://depts.washington.edu/nucmed/IRL/pet_intro/.